JOURNAL OF GEOPHYSICAL RESEARCH, VOL. 102, NO. B2, PAGES 2789–2806, FEBRUARY 10, 1997

Relative motions of the Pacific, Rivera, North American, and Cocos plates since 0.78 Ma

Charles DeMets

Department of Geology and Geophysics, University of Wisconsin, Madison

Douglas S. Wilson

Department of Geological Sciences, University of California, Santa Barbara

Abstract. We use magnetic anomaly and fracture zone crossings from 3°N-24°N along the East Pacific Rise to define the boundaries and relative velocities of the rigid Pacific, Rivera, North American, and Cocos plates since 0.78 Ma and to test several hypotheses regarding the nature of deformation between these plates. Crossings of the 0.78 Ma isochron from the Pacific-Rivera rise north of 22.0°N are significantly better fit by the 0-0.78 Ma Pacific-North America rotation than by a Pacific-Rivera rotation, thereby supporting a recently proposed model for accretion of the northern part of the Rivera plate to North America. A significant misfit of the Pacific-Cocos rotation to crossings of anomaly 1n from the East Pacific Rise north of 16.4°N suggests that seafloor north of ~16°N moves relative to the rigid Pacific or Cocos plates. We also find that nine crossings of the eastern Rivera fracture zone and eight crossings of anomaly 1n flanking the Manzanillo spreading segment are fit well by a Pacific-Rivera rotation. The Rivera-Cocos angular velocity derived from the best fitting Pacific-Cocos and Pacific-Rivera angular velocities predicts 19±3 mm yr^{-1} (95% confidence limit) of ~N-S convergence near the center of the Rivera-Cocos boundary. Nearby left-lateral, strike-slip earthquakes with north trending fault planes suggest that convergence is accommodated via sinistral shear along a north trending zone. The unambiguous kinematic and seismologic evidence for significant Rivera-Cocos motion indicates that the absence of a well-defined Rivera-Cocos plate boundary cannot be interpreted as evidence that Rivera-Cocos motion is slow or zero, as is postulated in several previous studies. The Rivera-Cocos angular velocity predicts oblique Rivera-Cocos convergence at the El Gordo graben and beneath the Manzanillo trough and southern Colima graben. Any extension across these features since 0.78 Ma thus cannot have resulted from divergence between the subducting Rivera and Cococs plates.

Introduction

The quantification of large-scale crustal movements on the surface of the Earth ranks as one of the most important accomplishments of the earth sciences in the twentieth century. Rigorously derived plate velocity models not only predict far-field plate velocities that are commonly used as constraints in models of deformation across wide plate boundaries [e.g., *McKenzie and Jackson*, 1983; *Haines and Holt*, 1993] but also enable hypothesis testing by dint of the uncertainties that accompany such models. Improvements in the accuracy and precision of plate kinematic models have been driven by the availability of more and higher-quality observations and through improvements in the techniques for defining best fitting and closure-consistent plate rotations [*Chase*, 1972; *Hellinger*, 1979], advances in techniques for treating data and model uncertainties [e.g., *Stock and Molnar*, 1983; *Chang*, 1988; *Chang et al.*, 1990; *Richardson and Cole*, 1991; *Wilson*, 1993a], new techniques for identifying rigid plate boundaries and plate circuit nonclosures [*Stein and Gordon*, 1984; *Gordon et al.*, 1987], and the reduction of random and systematic errors in the geomagnetic reversal timescale [*e.g. Baksi*, 1993; *Hilgen*, 1991].

Herein, we apply many of the above techniques to the numerous magnetic anomaly and fracture zone crossings that record 0-0.78 Ma seafloor spreading along the East Pacific Rise north of 3°N, the Pacific-Rivera rise, and the Gulf rise in the southern Gulf of California (Figure 1). Our goals are to test several unanswered questions about deformation within the Pacific, Cocos, Rivera, and North American plates that bear on their rigid plate geometries, and to construct a set of rotations that best describe their relative velocities since 0.78 Ma. We first examine whether the Rivera plate north of ~22.0°N accreted to the North American plate sometime during the past 1-2 million years [*Lonsdale*, 1995] and use anomaly crossings flanking the Tamayo fracture zone to estimate an upper bound for any remaining slip across this feature. We then test whether the enigmatic Manzanillo

Paper number 96JB03170.
0148-0227/97/96JB-03170$09.00

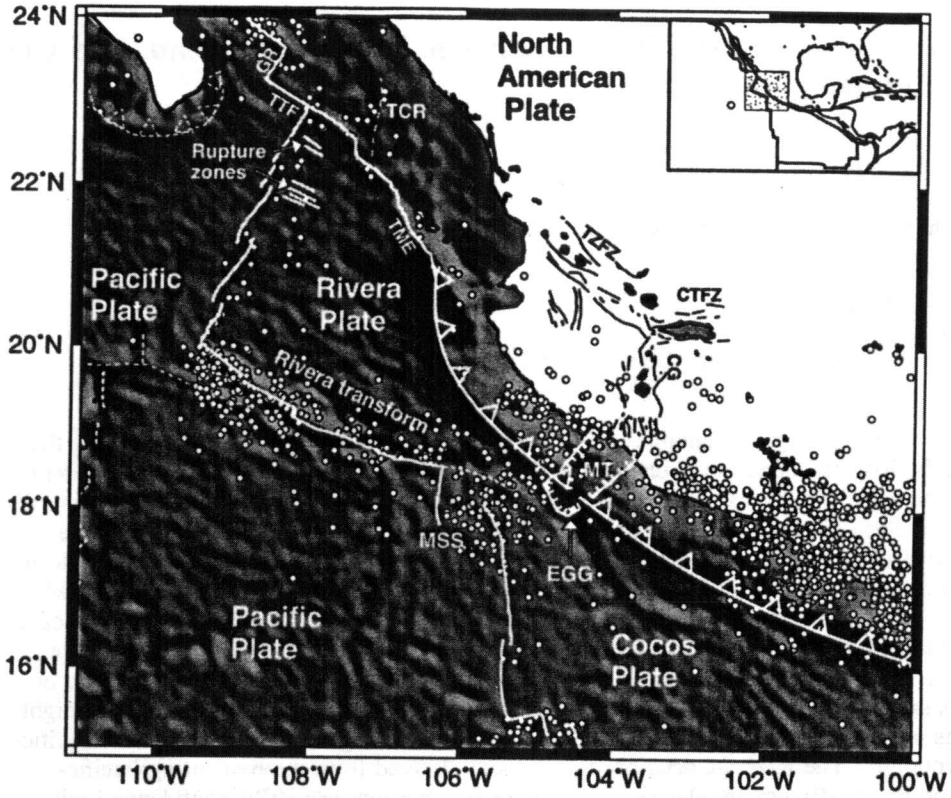

Figure 1. Principal features described in text and earthquakes shallower than 60 km depth for the period January 1967 to August 1996. Abbreviations are MSS, Manzanillo spreading segment; MT, Manzanillo trough; TCR, Tamayo Canyon rift; GR, Gulf rise; TTF, Tamayo transform fault; TME, Tres Marias escarpment; CG, Colima Graben; CTFZ, Chapala-Tula fault zone; TZFZ, Tepic-Zacoalco fault zone; EGG, El Gordo graben. The Rivera transform fault is digitized from *Ness and Lyle* [1991], *Bandy* [1992], and *Lonsdale* [1995], and the Tamayo Canyon rift follows *Ness and Lyle* [1991]. Solid and dashed lines designate active and inactive tectonic features, respectively. Marine gravity is illuminated from the southwest and is derived from the 2-km-gridded global marine gravity grid [*Smith and Sandwell*, 1995].

spreading segment is part of the Pacific-Cocos, Pacific-Rivera, or neither plate boundary. Finally, we revisit the question of whether seafloor spreading along the northern East Pacific rise is significantly slower than predicted by a rigid Pacific-Cocos rotation. *DeMets et al.* [1990] and *Wilson* [1993b] have previously reported misfits to magnetic anomaly crossings from the northern East Pacific rise, thereby implying that the Cocos or possibly Pacific plate is deforming in this region.

The need to examine these questions and derive new rigid plate rotations using appropriately modified geometries for the Rivera and Cocos plates is an important motivation for this work. Two additional factors also contribute to our reexamination of 0.78 Ma Rivera plate kinematics. One is the need for an accurate and precise model of Rivera and Cocos plate velocities where these plates subduct beneath North America. Such velocities are essential for attempts to understand interseismic strain buildup along the Middle America trench, which has spawned dozens of M=7+ earthquakes during this century [*Singh et al.*, 1985; *Anderson et al.*, 1989]. Geodetic measurements of Rivera plate motion relative to the surrounding plates are not presently feasible because the Rivera plate is located entirely beneath water.

Our second motivation is the lack of consensus regarding the nature of present-day motion between the Rivera and Cocos plates. Two classes of models for Rivera-Cocos motion now exist in the literature, one of which predicts significant motion between the Rivera and Cocos plates along their poorly defined boundary [*Nixon*, 1982; *Eissler and McNally*, 1984; *DeMets and Stein*, 1990; *Bandy*, 1992; *Lonsdale*, 1995], and the other of which presumes little or no relative motion other than slow divergence along the El Gordo graben (Figure 1) [*Bandy*, 1992; *Bandy and Pardo*, 1994; *Kostoglodov and Bandy*, 1995]. The former, which relies on inversion of seafloor spreading rates and plate slip directions to solve for the relative velocity of the Rivera and Cocos plates, predicts that the Rivera and Cocos plates converge at rates of ~20 mm yr^{-1} just west of the Manzanillo trough (Figure 1). When applied to areas elsewhere around the globe, this approach has yielded plate velocities that match geodetically measured velocities to within several percent [*DeMets et al.* 1990; *Smith et al.*, 1990]. The principal evi-

dence for models that postulate little or no Rivera-Cocos motion in the vicinity of their plate boundary is the absence of evidence from detailed shipboard surveys for a major throughgoing fault that could accommodate such motion [*Bourgois et al.*, 1988a; *Bandy*, 1992].

Our analysis differs from prior work as follows: (1) marine magnetic observations from the entire area of interest (3°N-24°N) are examined systematically and uncertainties in anomaly crossings are calibrated to reflect both navigational quality and the data dispersions, (2) rotations are derived from discrete crossings of seafloor spreading magnetic lineations and fracture zones [*Hellinger*, 1979], which permits us to more fully exploit existing data than do previous studies, (3) rigorous techniques are used to define the edges of the rigid Cocos and Rivera plates and to examine whether anomaly crossings from the recently discovered Manzanillo spreading segment [*Bourgois et al.*, 1988b], which terminates the eastern Rivera transform fault, record either Pacific-Rivera or Pacific-Cocos motion, and (4) Monte Carlo sampling techniques are used to estimate bounds on motion between the Rivera and Cocos plates, residual slip along the eastern Tamayo fracture zone, and the rate of internal Rivera or Pacific plate deformation near the Manzanillo spreading segment.

Data

We use the following data to estimate velocities since 0.78 Ma (which corresponds to the old edge of anomaly 1n according to *Cande and Kent* [1995]): (1) 14 crossings of anomaly 1n from the Gulf rise in the southern Gulf of California [*DeMets*, 1995], (2) 123 crossings of anomaly 1n from the Pacific-Rivera rise [*Traylen*, 1995], (3) 182 crossings of anomaly 1n between 17.3°N and 2.8°N along the Pacific-Cocos rise (D. Wilson, "Post-3 Ma Pacific-Cocos-Nazca Motion", manuscript in preparation, 1996), (4) eight crossings of anomaly 1n flanking the Manzanillo spreading segment, and (5) 25 crossings of the Clipperton, Siqueiros, and eastern Rivera fracture zones that approximate the chron 1n paleotransform configurations. We derived the anomaly crossings in categories 1-3 from original magnetic anomaly observations from more than 100 archived cruises; these are described in more detail in the above references. Data in categories 4 and 5 are described below.

The Manzanillo Spreading Segment

The Manzanillo spreading segment extends south from the eastern Rivera transform fault (Figure 1) [*Bourgois et al.*, 1988b] and is offset ~50 km west from the northernmost East Pacific Rise (Figure 2). The segment is propagating southwards [*Bourgois et al.*, 1988b; *Bandy and Hilde*, 1996] and has progressively decapitated the spreading axis to the east [*Bandy*, 1992]. The width of anomaly 1n, the positive magnetic anomaly centered on the rise axis (Figure 2), increases to the north until ~18.3°N, after which it remains nearly constant. North of 18.3°N, a comparison of the anomaly profiles with a synthetic magnetic anomaly profile (Figure 2) suggests that the old edge of anomaly 1n and the Jaramillo normal polarity anomaly are preserved on both sides of the rise axis, thereby indicating that seafloor spreading has been active along this part of the spreading segment since at least 0.78 Ma. To test whether spreading along the northernmost part of the Manzanillo spreading segment is consistent with either 0-0.78 Ma Pacific-Rivera or Pacific-Cocos spreading, we selected eight crossings of anomaly 1n that lie north of 18.3°N and are approximately equidistant from the Rivera fracture zone (Figure 2).

Fracture Zone Crossings and Conjugate Points

To constrain 0-0.78 Ma slip directions, we interpreted 0.78 Ma paleotransform positions for the Clipperton, Siqueiros, and eastern Rivera fracture zones from multibeam bathymetry, side-scan sonar, and where necessary, wide-beam bathymetry. Swath mapping images of these well-defined paleotransforms [*Gallo et al.*, 1986; *Bourgois et al.*, 1988b; *Fornari et al.*, 1989; *Macdonald et al.*, 1992; *Bandy and Hilde*, 1996] provide a strong basis for establishing the paleotransform configurations. Overall, we use 25 discrete fracture zone picks from these three fracture zones.

We also use conjugate points to constrain paleo-opening directions at several stages of the analysis, although none are used to constrain the best fitting rotations (Table 1). Conjugate points, which are defined as two points that originated at the same location along a paleospreading center, provide a convenient way to constrain finite opening directions if reliable fracture zone crossings are not available [*Wilson*, 1993a]. Any rotation that superimposes two conjugate points must be equidistant from those points, thereby constraining one of the three rotation parameters. We determined conjugate pairs by assuming that the post-0.78 Ma opening direction is adequately represented by averaging directions normal to the present rise axis and chron 1n.

Data Uncertainties

We assigned uncertainties to the locations of the fracture zone and magnetic anomaly crossings in two stages. In the initial, more subjective stage, we assigned uncertainties that reflected our judgement of the reliability of individual crossings. For the fracture zone crossings, we assigned conservative uncertainties of 1.0-2.5 km to account for the ambiguity that is involved in selecting the part of a fracture zone valley that represents a paleotransform fault. No further adjustment was made to these uncertainties. For the magnetic anomaly crossings, the 1-3 km uncertainties we assigned were based primarily on the quality of the underlying navigation.

We further adjusted the uncertainties in the magnetic anomaly crossings to ensure that they accurately reflect the dispersion of the anomaly crossings about the great circle segments associated with their best fitting rotations. Ideally, N observations that are fit by a model with m adjustable parameters should have a normalized least squares misfit χ^2 of approximately $N-m$ provided that the model is correctly parameterized, the assigned data uncertainties are approximately correct, and data residuals are approximately Gaussian. Using our initially assigned uncertainties, the anomaly crossings we use to solve for the best fitting Pacific-Cocos and Pacific-Rivera rotations have respective values of 0.653 and 0.577 for χ^2_ν (i.e., χ^2 divided by $N - m$). The original uncertainties are thus too large by respective factors of 1.24 and 1.32 ($1/\sqrt{\chi^2_\nu}$) and are divided by these factors to ensure that $\chi^2_\nu = 1.0$ for each set of anomaly crossings. None of the conclusions described below depend on this

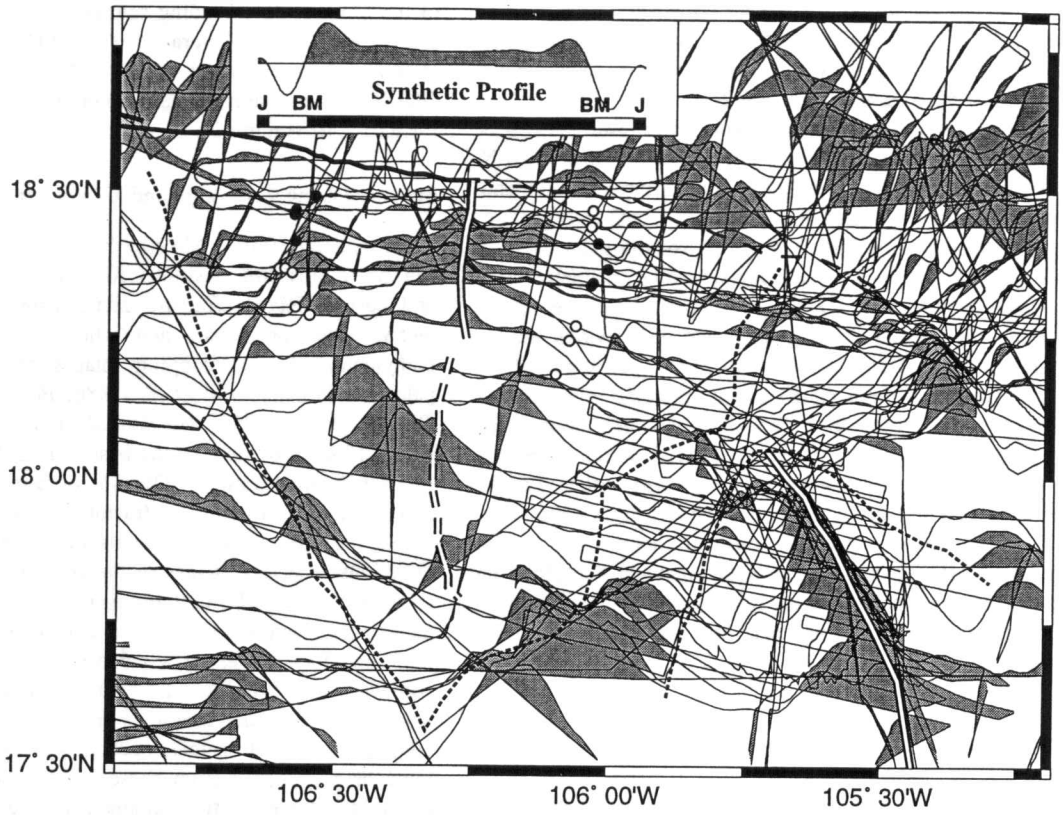

Figure 2. Marine magnetic anomalies along the Manzanillo spreading segment and northern East Pacific Rise. The inset shows a synthetic magnetic anomaly profile (inset) computed using magnetic parameters appropriate for the Manzanillo segment. The Brunhes-Matuyama reversal (BM in the inset) represents the old edge of anomaly 1n, which is the shaded positive anomaly. Solid circles show crossings of the old edge of anomaly 1n used to solve for Pacific-Rivera motion. All circles mark the edge of normally magnetized seafloor created by spreading during the Brunhes magnetic polarity epoch (e.g., anomaly 1n). Solid lines show the eastern Rivera transform fault and the rise axis [*Bourgois et al.* 1988a]. Locations of the eastern Rivera fracture zone (long dashed line) and wakes of the propagating rifts (short dashed lines) are from *Bandy and Hilde* [1996]. Abbreviation is J, Jaramillo normal polarity anomaly.

recalibration, but it is nonetheless useful to ensure that the model uncertainties reflect the dispersion of the data about the model predictions.

Techniques

Finite rotations and their covariances are derived using a general method for finding the rotation that best reconstructs magnetic anomaly and fracture zone crossings that define a paleospreading center [*Hellinger*, 1979; *Chang*, 1988]. Magnetic anomaly and fracture zone crossings are first grouped into a series of paleospreading and paleotransform segments and are assigned to a fixed or moving plate. The best fitting rotation is then defined as the rotation that minimizes the least squares scatter (χ^2) of the fixed and rotated observations from the great circle segments that best fit those observations. Three adjustable parameters are required to characterize the rotation that reconstructs data from the moving plate onto the fixed plate, and two parameters are required to describe each of the s great circle segments that best fit groups of reconstructed anomaly or fracture zone crossings. Optimizing the fit thus requires adjustment of $2s + 3$ parameters. Descriptions of the technique and the derivation of statistically rigorous rotation covariances are given by *Hellinger* [1979], *Chang* [1988], and *Royer and Chang* [1991].

Throughout the text, we use 0.78 Ma average plate velocities to approximate present-day plate velocities. We describe the present-day velocities of the Cocos, Rivera, and North American plates relative to the Pacific plate using angular velocity vectors that are constructed by dividing the Pacific-Cocos, Pacific-Rivera, and Pacific-North America finite rotation angles by 0.78 Ma. These angular velocities are summed vectorially to derive angular velocities that describe motion between the Rivera, North American, and Cocos plates. The uncertainties are propagated directly from the data and thus do not reflect additional uncertainties from the imperfectly known age of the old edge of anomaly 1n and biases that might result from outward displacement of magnetic reversal boundaries [*Atwater and Mudie*, 1973]. However, neither of these potential error sources is likely to change our rotations significantly: the age of the Brunhes-Matuyama reversal (i.e. the old edge of anomaly 1n) is probably known to better than 0.01 Ma [e.g. *Shackleton et al.*, 1990; *Baksi et al.*, 1992; *Bassinot et al.*, 1994], and the observed outward displacement of the Brunhes-Matuyama reversal boundary at 21°N along the Pacific-Rivera rise is

Table 1a. Finite Rotations

Plate Pair	Lat. °N	Long. °W	Angle, deg.	N	s	χ^2_ν
Pacific-Rivera	25.9	104.8	3.877	86	5	0.948
Pacific-Cocos	39.1	110.0	1.501	171	12	0.932
Pacific-N. America*	48.7	78.2	0.629			
Rivera-N. America	21.3	108.0	-3.352			
Cocos-Rivera	17.9	101.8	2.446			
Cocos-N. America	29.3	124.9	-0.965			

Rotations restore the first plate to its position with respect to the second plate at 0.78 Ma. Conversion to angular velocities requires dividing the rotation angle by 0.78 Ma. Reduced chi-square (χ^2_ν) is the least squares misfit χ^2 divided by the degrees of freedom ν, which equals N-2*s-3 [*Chang*, 1988].

* From *DeMets* [1995]

only ~250-500 m, about 1% of the total width of seafloor that has accreted since 0.78 Ma [*Macdonald et al.*, 1983].

We employ a variety of techniques for finding the limits of the rigid Rivera, Cocos, and Pacific plates where they flank the Pacific-Rivera and Pacific-Cocos rises. All of the techniques rely on comparison of the fits of one- and two-rotation models using the F test for additional terms [*Bevington and Robinson*, 1992]. Further details are provided below.

Geographic Limits of the Rigid Rivera Plate

Studies of Rivera plate kinematics published before 1995 assume that the northwestern boundary between the Rivera and North American plates coincides with the eastern Tamayo fracture zone. However, *Lonsdale* [1995] proposes that part of the Rivera plate accreted to North America sometime after ~1.5 Ma and that the present Rivera-North America boundary coincides with two recently discovered zones of normal faults extending southeast from near the Pacific-Rivera rise at 22.0°N and 22.5°N (Figure 1). *Traylen* [1995] demonstrates that 54 crossings of anomaly 1n located between the Tamayo fracture zone and the southernmost rupture zone identified by Lonsdale are underrotated by as much as 6 km by a Pacific-Rivera rotation that is derived only from anomaly crossings located south of these rupture zones. The observed misfit is significant at the 99.8% confidence level, thereby requiring significant displacement between seafloor located north and south of the southernmost rupture zone since 0.78 Ma.

Here, we use 14 crossings of anomaly 1n from the Gulf rise northeast of the Tamayo fracture zone and 123 crossings of anomaly 1n from the Pacific-Rivera rise to test *Lonsdale*'s [1995] hypothesis. We assume that the location of the boundary between the Rivera and North American plates east of the rise axis is unknown and we compare the fits of a series of two-rotation models for hypothetical boundary locations that range from 21.5°N along the Pacific-Rivera rise to a location coincident with the Tamayo fracture zone (i.e., the conventionally assumed location). For each location, anomaly crossings northeast of the assumed boundary are fit by fixing the rotation axis to the NUVEL-1 Pacific-North America rotation pole [*DeMets et al.*, 1990] and solving for the rotation angle that minimizes χ^2 for the fixed and rotated anomaly crossings. Anomaly crossings southwest of the hypothetical plate boundary are fit by solving for the Pacific-Rivera rotation that best reconstructs the anomaly crossings and a conjugate pair that enforces 0-0.78 Ma ridge-normal opening. The cumulative χ^2 for the two rotations is the measure of misfit [*Stein and Gordon*, 1984].

Rivera-North America boundary locations located at 21.5°N, 22.0°N, 22.5°N, and the Tamayo transform fault give respective least squares misfits of 78.5, 74.5, 79.8, and 90.0. The 137 anomaly crossings are thus best fit when the Rivera-North America boundary is assumed to intersect the Pacific-Rivera rise axis in the vicinity of the southernmost rupture zone, which intersects the rise axis at ~22.0°N. In this geometry, 69 of the 123 crossings of anomaly 1n lie south of 22.0°N and thus record Pacific-Rivera motion.

The values of χ^2 for the hypothetical boundaries at 21.5°N, 22.5°N, and the Tamayo fracture zone exceed χ^2 for the best fitting geometry at respective risk levels of 1%, 0.4%, and 2 ppm according to an F test for one additional term (the boundary location). A geometry in which the northern limit of rigid Pacific-Rivera motion coincides with the rupture zone at

Table 1b. Rotation Covariances

Plate Pair	a	b	c	d	e	f	g
Pacific-Rivera	1.493	5.029	-1.812	17.085	-6.124	2.205	10^{-6}
Pacific-Cocos	0.418	0.774	-0.144	2.799	-0.607	0.140	10^{-7}
Pacific-N. America	1.194	-0.335	0.319	2.496	-1.720	3.031	10^{-8}
Rivera-N. America	1.447	4.943	-1.756	17.211	-6.099	2.192	10^{-6}
Cocos-Rivera	1.439	4.953	-1.774	17.443	-6.224	2.236	10^{-6}
Cocos-N. America	0.537	0.742	-0.113	3.045	-0.779	0.447	10^{-7}

Covariances describe the uncertainty in the reconstructed location of the first plate relative to the second plate. Covariances are Cartesian, with elements a, d, and f representing the variances of the (0°N, 0°E), (0°N, 90°E), and 90°N components of the best fitting rotation [*Chang*, 1988; *Chang et al.*, 1990; *Royer and Chang*, 1991]. Covariances have units of square of radians. The covariance matrices are reconstructed as follows:

$$\begin{pmatrix} a & b & c \\ b & d & e \\ c & e & f \end{pmatrix} \cdot g$$

Table 1c. Angular Velocities and Covariances

Plate Pair	Latitude °N	Longitude °W	ω, deg/Myr	*a*	*b*	*c*	*d*	*e*	*f*	*g*
Rivera-N. America	21.4	108.2	4.30	2.47	8.26	-2.97	2.81	-10.10	3.67	10^{-6}
Rivera-Cocos	17.8	102.1	3.14	0.25	0.84	-0.30	2.85	-1.02	0.36	10^{-5}
Cocos-N. America	29.4	125.1	1.24	0.88	1.22	-0.18	5.01	-1.28	0.73	10^{-7}

Angular velocities express the present-day motion of the first plate relative to the second plate. Angular velocities are derived by summing the Pacific-Rivera, Pacific-Cocos, and Pacific-North America angular velocities (i.e., the finite rotations with the angles divided by 0.78 Myr and covariances divided by the square of 0.78 Myr).

22.0°N thus fits the observations significantly better than alternative geometries.

We also tested a geometry in which the North American plate extends all the way to the Rivera transform fault, which is tantamount to assuming complete suture of the Rivera plate to North America. This geometry gives χ^2 of 354.3, roughly a fivefold increase from χ^2 for the best fitting geometry. The increase in χ^2 is significant at 4 parts in 10^{42}. Figure 3 underscores this result: the central anomaly along the southern Pacific-Rivera rise is ~5-10 km wider than predicted by the 0-0.78 Ma Pacific-North America rotation. The data thus clearly exclude a model in which the entire Rivera plate ceased moving relative to North America after 0.78 Ma.

Bounds on Residual Slip Across the Eastern Tamayo Fracture Zone

The above result indicates that the North American plate extends southwest of the eastern Tamayo fracture zone, which implies that this fault should be seismically inactive. However, seismicity along the eastern Tamayo fracture zone (Figure 1) indicates that it still accommodates some motion. To estimate an upper bound for this slip, we apply Monte Carlo sampling techniques to 14 Gulf rise anomaly crossings that record opening rates just north of the Tamayo fracture zone and 54 anomaly crossings located between the Tamayo fracture zone and southern rupture zone at ~22.0°N. The Monte Carlo method is a robust statistical technique for determining how much an estimated parameter changes when the data that are used to estimate this parameter are randomly perturbed within bounds specified by their assumed probability density functions [*Bevington and Robinson*, 1992].

Estimating the bounds on slip along the eastern Tamayo fracture zone requires several steps. We first approximate the probability density functions for the 68 anomaly crossings as Gaussian with 1σ widths equal to their assigned, recalibrated uncertainties. We then perturb each anomaly crossing in a direction parallel to the opening direction and by a distance equal to its assigned uncertainty multiplied by a random number drawn from a Gaussian distribution with a mean of 0.0 and a standard error of 1.0. We repeat this process 1000 times for each anomaly crossing, thereby creating 1000 sets of 68 randomly perturbed anomaly crossings.

Since the 0-0.78 Ma slip directions immediately north and south of the Tamayo fracture zone are both parallel to the Pacific-North America direction [*Lonsdale*, 1995], any motion across the fracture zone must parallel the Pacific-North America direction and result from different angular opening rates north and south of the Tamayo transform fault. For each of the 1000 data sets, we thus fix the rotation axes for the 14 anomaly crossings north of and 54 anomaly crossings south of the Tamayo transform fault to the NUVEL-1 Pacific-North America pole and we solve for the rotation angles that separately best fit the the two sets of anomaly crossings. The resulting 1000 pairs of best fitting rotation angles are subtracted (since they share a common rotation axis) and the differential rotation is used to predict the rate of differential slip between seafloor north and south of the eastern Tamayo fracture zone at its intersection with the Pacific-Rivera rise (see star in Figure 3).

The resulting distribution of slip rates has a mean of 1.6 mm yr^{-1} and 95% upper bounds of 3.8 mm yr^{-1} of right-lateral slip and 0.7 mm yr^{-1} of left-lateral slip. Thus, although the data are consistent with a model in which no slip occurs, right-lateral slip as fast as 4 mm yr^{-1} could occur without emerging from the noise in the available data. We thus postulate that motion between the Rivera and North American plates is partitioned between the Tamayo fracture zone and the rupture zones to the south, with up to 4 mm yr^{-1} of fault-parallel slip causing the continued seismicity along the Tamayo fracture zone.

Geographic Limits of the Rigid Cocos Plate

Previous studies of present-day seafloor spreading rates along the Pacific-Cocos spreading center suggest that spreading north of the Orozco transform fault is several millimeters per year slower than predicted by best fitting and closure-enforced Pacific-Cocos rotations, thereby implying that the Cocos or possibly Pacific plate adjacent to the northern East Pacific Rise is deforming [*DeMets et al.*, 1990; *Wilson*, 1993b]. Using the 182 crossings of anomaly 1n from the Pacific-Cocos rise, we revisit the question of whether the width for anomaly 1n along the northern part of the Pacific-Cocos rise differs significantly from that predicted by a Pacific-Cocos rotation derived from crossings of anomaly 1n farther to the south. The uneven distribution of fracture zone crossings along the plate boundary prevents us from undertaking a similar examination of the along-axis opening directions.

Defining the southernmost spreading segment along the Pacific-Cocos rise (Figure 4) as segment 1, we systematically examine whether anomaly crossings flanking the *N*th spreading segment show any evidence for a significant departure from opening predicted by a rotation derived from segments 1 through *N*-1. To do so, we compare χ^2 for the rotation that simultaneously best fits data from segments 1 through *N* to the cumulative χ^2 for rotations that separately fit data from

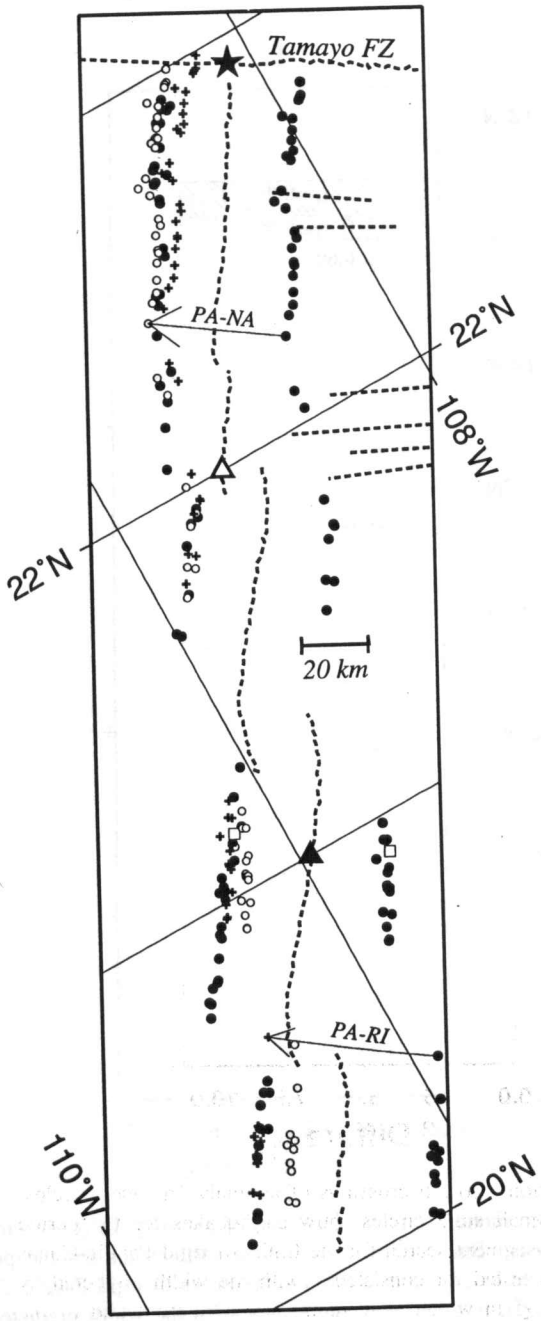

Figure 3. Crossings of the old edge of anomaly 1n east of the Pacific-Rivera rise rotated onto the Pacific plate by the Pacific-North America finite rotation (shown by open circles) and Pacific-Rivera finite rotation (shown by pluses). Solid circles show the unrotated crossings of anomaly 1n. The star shows the location where we estimate slip between seafloor north and south of the Tamayo fracture zone (see text). The open triangle shows the northernmost location of anomaly crossings that are used to constrain Pacific-Rivera motion, and the solid triangle designates the geographic center of Pacific-Rivera spreading. The open squares show the conjugate point locations. Dashed lines show the present-day Pacific-Rivera rise axis, Tamayo fracture zone, and rupture zones identified by *Lonsdale* [1995]. Anomaly crossings located north of the open triangle are systematically misfit by a rotation derived from anomaly crossings located south of the filled triangle, in accord with a model in which seafloor north of ~22°N has detached from the rigid Rivera plate [*Lonsdale*, 1995].

segment N and segments 1 through N-1. Data from the Nth segment, which by themselves contain too little information to solve for a unique rotation, are fit by solving for the opening angle and pole location subject to the restriction that the best fitting rotation predict ridge-normal opening. Because of this restriction, the two-rotation model has only two more adjustable parameters than does the one-rotation model. The significance of changes in χ^2 is thus evaluated using an F test for two additional terms.

Beginning with the spreading segment north of the Clipperton transform fault, the first significant departure from rigid Pacific-Cocos motion occurs for the spreading segment north of 16.4°N (Figure 4). From 16.4°N-17.0°N, anomaly 1n is 2.3±1.1 km (95%; hereafter, all quoted uncertainties are 95%) narrower than predicted by a rotation derived from all anomaly crossings south of 16.4°N. Crossings of anomaly 1n just north of the Orozco transform fault (Figure 4) show a marginally significant deficit of 1.1±1.8 km relative to the width predicted by a rotation derived from anomaly crossings south of the Orozco transform (Figure 4). The spreading deficit we observe north of the Orozco transform fault corroborates the deficit described by *DeMets et al.* [1990] and *Wilson* [1993b] and indicates that rigid Pacific-Cocos motion is not recorded by the spreading center north of the Orozco transform fault. Consequently, no anomaly crossings north of ~16.0°N are used to derive the Pacific-Cocos rotation.

The observed spreading deficit has at least two possible explanations. Motion between the Rivera and Cocos plates might be accommodated by seafloor deformation as far south as 16°N, although diffuse seismicity west of the Middle America trench is largely focused north of 17°N (Figures 1 and 4). If the 3±1.5 mm yr^{-1} spreading deficit north of 16.4°N is attributable to seafloor deformation east of the rise axis (e.g., distributed Rivera-Cocos motion), it implies westward motion of lithosphere north of 16.4°N relative to the rigid Cocos plate. Alternatively, eastward motion relative to a rigid Pacific plate is implied if deformation is focused west of the rise axis (e.g., residual slow spreading along the Mathematician ridge several hundred kilometers to the west). In either case, the spreading deficit records only one component of that deformation.

Tectonic Setting of the Manzanillo Spreading Segment

Although the Manzanillo spreading segment was discovered in 1987 [*Bourgois et al.*, 1988a], no definitive study of whether it belongs to the Pacific-Rivera, Pacific-Cocos, or neither plate boundary has been published. *Lonsdale* [1995] notes that a great circle passing through the Pacific-Rivera rotation pole parallels the trend of the Manzanillo spreading segment, thereby suggesting that spreading across the Manzanillo segment reflects Pacific-Rivera motion. Below, we test this hypothesis by comparing the 0-0.78 Ma opening distances and directions predicted by the Pacific-Rivera and Pacific-Cocos rotations to the opening distances and directions defined by crossings of anomaly 1n and bathymetric lineaments mapped from detailed bathymetric and side-scan sonar surveys of seafloor flanking the Manzanillo spreading segment. In a related vein, we also examine whether 0-0.78 Ma crossings of the eastern Rivera fracture zone are adequately reconstructed by a Pacific-Rivera rotation

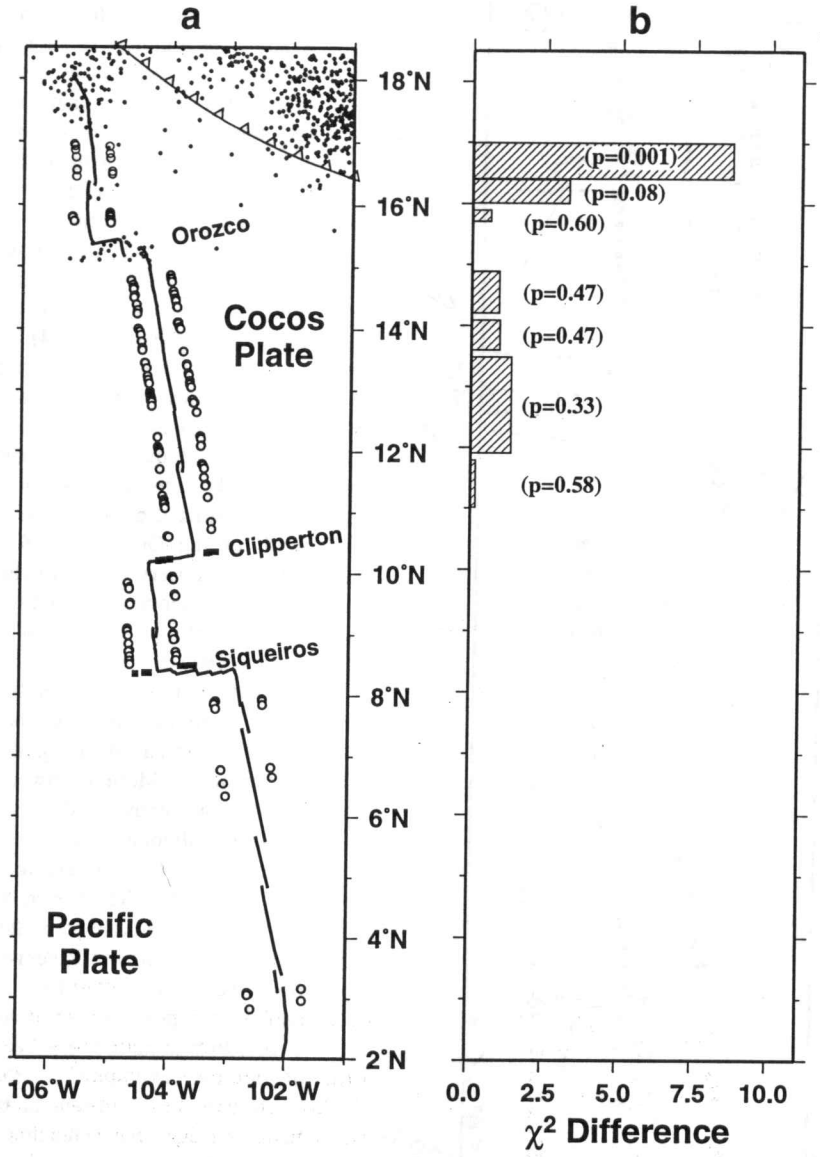

Figure 4. Search for the limits of rigid Pacific-Cocos motion. (a) All crossings of anomaly 1n (open circles) and fracture zones (solid squares) used in the analysis. Small solid circles show earthquakes for the period January 1967 to August 1996. (b) Results of a segment-by-segment search for the limits of rigid Pacific-Cocos motion. For a given segment, the width of anomaly 1n is tested for consistency with the width predicted by segments to the south. Bars show the difference between χ^2 in which all data from the southern end of the Pacific-Cocos rise through a given segment are fit with a single rotation and χ^2 in which data from a given segment and all segments to the south are fit with separate rotations. Probabilities p that are smaller than 0.05 indicate that the change in χ^2 for a one- versus a two-rotation model is less than 5% probable for an internally consistent set of anomaly crossings with normally distributed errors. The probabilities are determined using the F ratio test. Details are given in the text.

that is derived only from data along the Pacific-Rivera spreading center several hundred kilometers to the northwest.

Tests for Consistency With Pacific-Rivera and Pacific-Cocos Motion

We use both a visual and statistical test to determine whether kinematic observations from the Pacific-Rivera rise, the eastern Rivera fracture zone, and the Manzanillo spreading segment can be fit with a single rotation. Four crossings of anomaly 1n west of the Manzanillo segment and five Rivera fracture zone crossings, when rotated into a fixed Pacific plate reference frame using a rotation derived solely from 69 anomaly crossings and two conjugate points from the Pacific-Rivera rise south of 22.0°N, are closely aligned with their fixed-side counterparts (Figure 5). Moreover, great circles that emanate from the Pacific-Rivera rotation pole accurately predict the trends of bathymetric lineaments defined by multibeam bathymetry and side-scan sonar [*Bourgois et al.*, 1988b; *Bandy and Hilde*, 1996; K. Macdonald, unpublished data, 1995] (Figure 5). The observations are thus visually consistent with the hypothesis that the Manzanillo spreading segment has recorded Pacific-Rivera motion since 0.78 Ma.

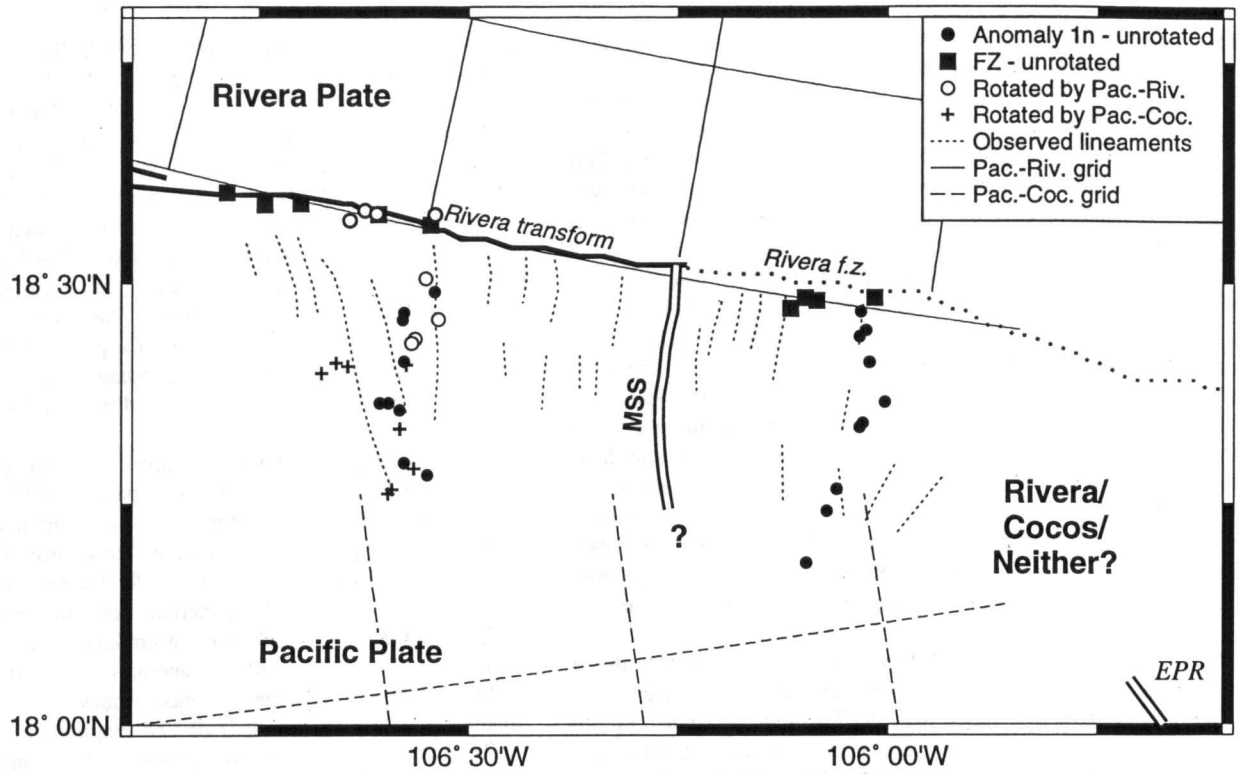

Figure 5. Test for the tectonic setting of the Manzanillo spreading segment (MSS). The thin solid lines are small circles about or great circles through a Pacific-Rivera pole that is derived only from Pacific-Rivera rise anomaly crossings and a conjugate pair that enforces ridge-normal opening. Long dashed lines are a similar grid about the Pacific-Cocos best fitting rotation. Both rotations do a good job of reconstructing the crossings of anomaly 1n on the Pacific plate; however, only the grid about the Pacific-Rivera rotation fits the Manzanillo rise axis (bold line) and bathymetric lineaments interpreted from swath maps.

If we use the Pacific-Cocos rotation to rotate the four Manzanillo segment anomaly crossings into a fixed Pacific plate reference frame, we observe a worse alignment of the reconstructed data (Figure 5). The reconstructed anomaly crossings are well aligned (Figure 5); however, great circles that emanate from the Pacific-Cocos rotation pole differ by 15° or more from the trends of the present rise axis and bathymetric lineaments south of the Rivera fracture zone (Figure 5). The observations are thus visually inconsistent with the hypothesis that spreading along the Manzanillo segment records Pacific-Cocos motion. This result is not unexpected given our prior conclusion that the northern limit of rigid Pacific-Cocos motion is ~16°N.

To test rigorously the hypothesis that 0-0.78 Ma motion along the Manzanillo segment and eastern Rivera fracture zone is consistent with that predicted by the Pacific-Rivera rotation, we examine whether one or two rotations are required to fit the 69 anomaly crossings and one conjugate pair that record Pacific-Rivera motion and the eight Manzanillo segment anomaly crossings and nine eastern Rivera fracture zone crossings. Fitting all 88 observations with one rotation gives $\chi^2 = 41.6$. In contrast, fitting the 71 Pacific-Rivera rise data and the 17 other observations with separate rotations gives χ^2 of 40.3. An F test indicates that the decrease in χ^2 caused by fitting the observations with an additional rotation is not significant. All of the data are thus consistent with a model in which opening across the Manzanillo segment and slip along the eastern Rivera fracture zone record motion between the Pacific and Rivera plates.

In the ensuing analysis, we thus solve for Pacific-Rivera motion using the 69 Pacific-Rivera magnetic anomaly crossings and the 17 data from the eastern Rivera fracture zone and Manzanillo spreading segment. However, none of the results and conclusions described below are sensitive to our use of the latter data. For example, excluding the eight Manzanillo segment anomaly crossings while solving for Pacific-Rivera motion results in only minor (<10%) increases in the uncertainties and small (e.g., < 0.5 mm yr^{-1} and 0.5°) changes in the velocities of the Rivera plate with respect to the Pacific, Cocos, and North American plates.

An Upper Bound on Seafloor Deformation East and West of the Manzanillo Spreading Segment

The results described above indicate that any motion between seafloor flanking the Manzanillo spreading segment and the rigid Rivera or Pacific plates is slower than some threshold whose value depends on the uncertainties we assigned to the anomaly crossings. To determine the value of this threshold and thus estimate the maximum rate at which seafloor just east or west of the Manzanillo segment can move with respect to either the rigid Rivera or Pacific plates, we apply the Monte Carlo sampling technique to the 69 Pacific-Rivera and eight Manzanillo segment anomaly crossings. We estimate only an upper bound on motion parallel to the eastern Rivera transform fault and assume that any transform-orthogonal motion, which would require

oblique spreading along the Manzanillo spreading segment, is slow enough to be ignored.

Using procedures described above, we randomly perturbed the locations of the Pacific-Rivera and Manzanillo segment anomaly crossings within bounds specified by their probability density functions and assembled 1000 pairs of data sets, one consisting of 69 Pacific-Rivera anomaly crossings and the other consisting of eight Manzanillo segment anomaly crossings. We then solved for the rotation that best fit a given set of Pacific-Rivera anomaly crossings and used the resulting rotation axis to solve for the rotation angle that best fit a set of eight Manzanillo segment anomaly crossings. Finally, we subtracted the two angles for the coincident rotation axes and used the differential rotation to predict the difference between post-0.78 Ma Pacific-Rivera and Manzanillo segment spreading rates at the northern end of the Manzanillo segment (18.5°N, 106.25°W). To ensure that all of the rotations predict motion parallel to the eastern Rivera transform fault, the Pacific-Rivera anomaly crossings were always inverted with the nine eastern Rivera fracture zone crossings.

The 1000 resulting differential rates indicate that the 0-0.78 Ma spreading rate across the Manzanillo segment is 1.4±2.5 mm yr^{-1} faster than the Pacific-Rivera rate. Motion of the seafloor flanking the Manzanillo segment relative to either the rigid Rivera or Pacific plates is thus indistinguishable from no motion. For example, if we assume that slow slip along the Rivera fracture zone east of its intersection with the Manzanillo spreading segment decouples the rigid Rivera plate from seafloor east of the Manzanillo segment, these results impose 95% upper bounds of 4 mm yr^{-1} of left-lateral slip and 1 mm yr^{-1} of right-lateral slip. Alternatively, if we assume that residual extension along the northern Mathematician ridge causes seafloor south of the Rivera transform fault to move to the east relative to the rest of the Pacific plate, our results indicate that this extension cannot exceed 1 mm yr^{-1} .

Pacific, Rivera, Cocos, and North American Plate Motions Since 0.78 Ma

Using the plate geometries described above, we next solve for the rotations that best fit the Pacific-Rivera and Pacific-Cocos magnetic anomaly and fracture zone crossings and also determine the covariances that describe their uncertainties. Tables 1a and 1b list the best fitting rotations and covariances, which are useful for predicting total displacements since 0.78 Ma, and Table 1c gives angular velocities, which are more appropriate for describing 0.78 Ma average linear velocities. The Rivera-North America, Cocos-North America, and Rivera-Cocos rotations and covariances are derived using standard techniques for combining finite rotations and their covariances [e.g., *Royer and Chang*, 1991], and their corresponding angular velocities are derived through vector summation. The rotations and some of their tectonic implications are described below.

Pacific-North America

The 0-0.78 Ma Pacific-North America rotation was determined by fixing the rotation axis to the NUVEL-1 Pacific-North America pole location and solving for the angle that best reconstructed 14 crossings of anomaly 1n from the southern Gulf of California [*DeMets*, 1995]. The 0-0.78 Ma rotation predicts seafloor spreading of 51±2.5 mm/yr (all uncertainties quoted herein are 95%) along the Gulf rise. The 0.78 Ma average rate is ~8% faster than the 3.16 Ma average opening rate predicted by the NUVEL-1A model [*DeMets et al.*, 1994], but it agrees well with the 49-53 mm yr^{-1} opening rates determined from very long baseline interferometry [*Argus and Gordon*, 1990] and Global Positioning System measurements (K. Larson and J. Freymueller, Global plate velocities from the Global Positioning System, manuscript submitted to *Journal of Geophysical Research*, 1996). Possible reasons for the discrepancy between the 0.78 Ma and 3.16 Ma average rates are discussed by *DeMets* [1995].

Because separate data sets are inverted to solve for the rotation angle [*DeMets*, 1995] and pole [*DeMets et al.*, 1990], the covariances between these parameters are unknown. To approximate the rotation covariance matrix, we extracted the uncertainty in the pole location from the NUVEL-1A Pacific-North America rotation covariances [*DeMets et al.*, 1994] and the uncertainty in the rotation angle from the variance of the anomaly 1n rotation angle [*DeMets*, 1995]. We then assigned values of zero to all covariances that relate the latitude and longitude of the rotation to its angle, constructed the composite covariance matrix in a local coordinate system centered on the Pacific-North America rotation axis, and transformed the matrix back into the Cartesian coordinate system (Table 1b).

Pacific-Rivera

The rotation that best fits the 69 anomaly crossings from the southern three segments of the Pacific-Rivera rise, the nine crossings of the eastern Rivera fracture zone, and the eight anomaly crossings from the Manzanillo spreading segment (Table 1) lies south of previously derived rotations for 0-0.78 motion (Figure 6) [*DeMets and Stein*, 1990; *Bandy*, 1992; *Lonsdale*, 1995] and thus predicts a slightly steeper along-axis opening gradient than do prior models. Owing to our intentional decision to assign conservative uncertainties to the fracture zone crossings, χ^2_ν for the 86 observations is slightly smaller than 1.0 (Table 1).

A small circle about the new best fitting rotation axis parallels the trace of the Rivera transform fault (Figure 7) nearly everywhere along its length, thereby indicating that the present trace of the fault is consistent with transcurrent motion since 0.78 Ma. The new best fitting rotation predicts velocities that are similar to those predicted by previous models but with smaller uncertainties due to the larger numbers of data we use and our recalibration of the data uncertainties. For example, after adjusting all angular rotation rates to a common geomagnetic reversal timescale [*Cande and Kent*, 1995], the 0.78 Ma average Pacific-Rivera angular velocities derived here and by *DeMets and Stein* [1990], *Bandy* [1992], and *Lonsdale* [1995] predict velocities that differ by no more than 1.8 mm yr^{-1} and 6° (Table 2) near the geographic center of Pacific-Rivera spreading (solid triangle in Figure 3). Points that are rotated with the new best fitting rotation have uncertainty confidence ellipses that are 70% and 64% smaller than for points rotated using the anomaly 1n rotations from *DeMets and Stein* [1990] and *Bandy* [1992] respectively (no uncertainties are given by *Lonsdale* [1995]).

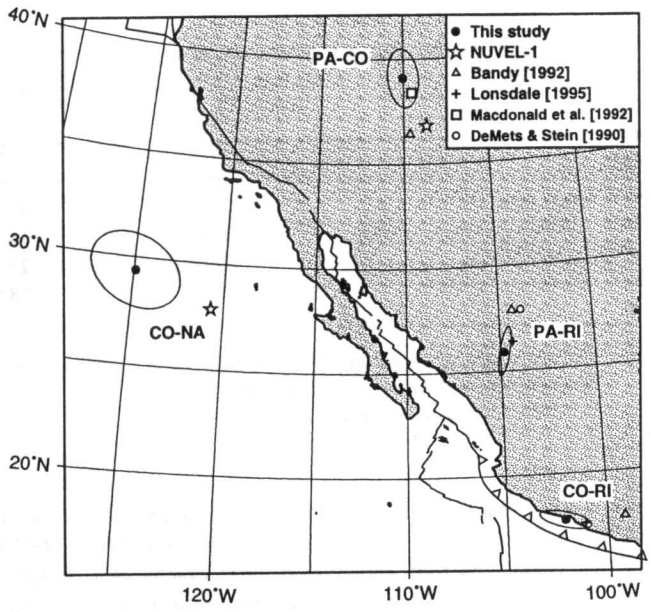

Figure 6. Summary diagram of rotation pole locations from this and prior studies. All ellipses are two-dimensional 95% confidence limits.

Pacific-Cocos

The best fitting Pacific-Cocos rotation is derived from 155 anomaly crossings along 10 spreading segments between 2.8°N and 16.0°N and 16 crossings of the Clipperton and Siqueiros fracture zones (Figure 4). The rotation axis lies significantly north of the 3.16 Ma average NUVEL-1A pole and the 0.78 Ma average pole derived by *Bandy* [1992] (Figure 6) and thus predicts a more gradual along-axis opening gradient than these models. About half of the northward shift in the pole relative to the NUVEL-1A pole location stems from our exclusion of the anomaly crossings north of 16.0°N. The remainder of the difference thus stems from possible changes in the Pacific-Cocos pole location since 3.16 Ma and the fact that we did not impose any plate circuit closure requirements on the Pacific-Cocos rotation. Relative to the 3.16 Ma average Pacific-Cocos velocity predicted by NUVEL-1A at 10°N along the spreading center, the 0.78 Ma average velocity predicted here is 4±2% faster and in the same direction.

Cocos-North America

The 0.78 Ma average Cocos-North America angular velocity derived here (Table 1c) differs from its NUVEL-1A counterpart in two important respects. First, the newly derived pole lies significantly farther west than does the NUVEL-1 pole (Figure 6). It thus predicts a smaller gradient in convergence rates along the trench. The westward shift results largely from the aforementioned northward shift of the Pacific-Cocos rotation axis (Figure 6). Perhaps more importantly, the newly derived angular velocity predicts 0-0.78 Ma convergence along the northern Middle America trench that is 12±5% (i.e., 5.4±2.3 mm yr^{-1}) faster than predicted by the 3.16 Ma NUVEL-1A Cocos-North America angular velocity.

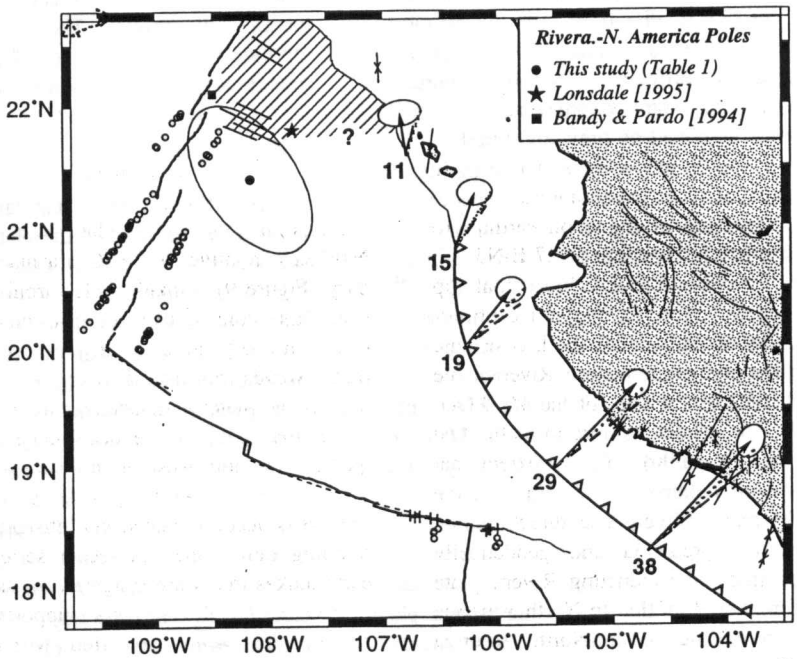

Figure 7. Rivera-North America velocities, pole locations, and 2-D 95% uncertainties. Solid arrows show velocities predicted at the vector origins by the best fitting 0.78 Ma Rivera-North America angular velocity. Convergence rates in millimeters per year are given at vector origins. Dotted and dashed vectors show the velocities predicted by the *Bandy and Pardo* [1994] and *Lonsdale* [1995] Rivera-North America anomaly 1n angular velocities, respectively. Dashed lines along the Rivera transform fault are small circles about the best fitting Pacific-Rivera rotation. Open circles and pluses show all crossings of anomaly 1n and fracture zone crossings used to derive the Pacific-Rivera rotation. Inward pointing arrows show the principal shortening axes of major thrust earthquakes along the coast for the period 1965-1996. Arrow lengths are scaled by the logarithm of the earthquake moment release.

This increase results from the fact that the 0-0.78 Ma Pacific-Cocos and Pacific-North America angular velocities both predict faster motion than do their 3.16 Ma average NUVEL-1A counterparts. The meaning of the apparent acceleration of Cocos-North America motion since 3.16 Ma is debatable. For example, *DeMets* [1995] proposes that the NUVEL-1A Pacific-North America angular velocity underestimates 3.16 Ma average Pacific-North America motion by several percent. If true, this implies that at least some of the apparent acceleration in Cocos-North America motion is an artifact of several percent inaccuracies in the NUVEL-1A model.

Table 2. Pacific-Rivera Predicted Velocities

Model	Rate, mm yr^{-1}	Azimuth, °CW
This study	60.4±0.7	127.4°±4.4
DeMets and Stein [1990]	60.5±1.9	123.0°±5.1
Bandy [1992]	60.1±1.5	121.0°±4.6
Lonsdale [1995]*	62.2	128.0°

All velocities are predicted at 21.0°N, 109.0°W. All uncertainties are one-dimensional 95%. CW, clockwise.

* No uncertainties accompany the model.

Rivera-North America

Combining the well-constrained Pacific-North America and Pacific-Rivera angular velocities yields a Rivera-North America angular velocity (Table 1c) that places strong bounds on the range of convergence velocities along the Rivera-North America plate boundary. The predicted velocities range from trench-normal convergence of 38±4 mm yr^{-1} at the southernmost limit of Rivera plate subduction to highly oblique underthrusting beneath the Tres Marias islands north of ~21°N (Figure 7). The velocity predictions are typically well constrained, with 95% rate uncertainties of ±3 mm yr^{-1} along much of the boundary and directional uncertainties decreasing from ±23° beneath the Tres Marias islands to only ±4° at the southern end of the plate boundary.

The predicted convergence rates (Figure 7) are similar to but have smaller uncertainties than the predictions of other recently published models [*Bandy and Pardo*, 1994; *Lonsdale*, 1995]. The predicted directions are systematically counterclockwise from directions predicted by previous models, with the largest differences occurring north of 20.75°N, where the predicted convergence is more oblique to the plate boundary than predicted by previous models.

The newly derived rotation has several interesting implications for deformation along the Rivera-North America plate boundary. Along the section of the trench ruptured by the October 9, 1995, M_w=8.0 Manzanillo subduction earthquake the predicted range of convergence directions (N27°E-N37°E) does not differ significantly from the N30°E±5° principal slip directions derived independently from the Harvard centroid-moment tensor solution and geodetically measured, coseismic displacements at 11 sites above the subducting Rivera plate (T. Melbourne et al., The geodetic signature of the *M*8.0 Oct. 9, 1995 Jalisco subduction earthquake, manuscript submitted to *Geophysical Research Letters*, 1996). To the extent that the strain released by this earthquake is representative of the long-term Rivera-North America convergence direction, the close agreement between the predicted and geodetically observed direction implies that the subducting Rivera plate transfers little or no margin-parallel motion to North America along the southern portion of the Rivera-North America boundary.

From 20°N to 21°N, the predicted convergence direction is highly oblique to the plate boundary (Figure 7), raising the possibility that convergence is partitioned between slow trench-normal motion and margin-parallel shear. For example, the velocity components normal and parallel to the north trending plate boundary at 20.75°N are 6±4 and 14±3 mm yr^{-1}. We speculate that the trench-parallel component is accommodated by one or more strike-slip faults landward of the trench, as is often the case in forearcs that lie above obliquely convergent boundaries [*Jarrard*, 1986; *McCaffrey*, 1992]. Marine geophysical observations that include Sea Beam swath bathymetry and single-channel seismic profiles in this region apparently reveal a strike-slip fault landward of the trench [*Bourgois et al.*, 1988a], although no data are presented with the maps that identify this fault. Some or all of the trench-parallel component of motion might also be accommodated through extension within the continent well inboard of the trench [*Kostoglodov and Bandy*, 1995].

North of 21°N, where the plate boundary bends to the northwest, two thrust earthquakes along the Tres Marias escarpment (2.9.76 in work by *Goff et al.* [1987] and 4.1.91 in work by *Pardo and Bandy* [1994]) suggest that the Rivera plate is still actively thrusting beneath or converging with the continental margin. The predicted convergence velocity is oblique to the margin and thus implies that partitioning into trench-normal and margin-parallel components might occur.

Rivera-Cocos

The Rivera-Cocos angular velocity, which is located several degrees east of the plate boundary (Figures 6 and 8b), predicts that the Cocos plate moves 19±3 mm yr^{-1} toward N10°E±6° relative to the Rivera plate along their plate boundary (Figure 9). Small circles around the Rivera-Cocos rotation axis indicate that the two plates converge in a ~N-S direction everywhere within the zone of distributed seismicity that extends northward from ~17-17.5°N and presumably defines the plate boundary (Figure 8a).

On the basis of the occurrence of two strike-slip earthquakes just northwest of the Manzanillo trough (Figure 8b), *Eissler and McNally* [1984] propose that Rivera-Cocos motion is accommodated via left-lateral motion along a north trending fault zone. A recent series of offshore strike-slip earthquakes that were triggered by the October 9, 1995, Manzanillo earthquake strongly supports such a model. These earthquakes, which occurred within the zone of diffuse seismicity between the Rivera and Cocos plates (Figure 8a), ruptured ~60 km of a north-northeast trending fault northwest of the Manzanillo trough (the earthquakes are shown as stars in Figure 8a). The earthquake sequence consisted of two *M* 4+ foreshocks on November 21, 1995, M_s = 5.7 and 5.6 main shocks on December 11, 1995, and several *M* 4-5 aftershocks on December 11 and 12, 1995. Harvard centroid-moment tensors for the two largest shocks and an earlier nearby earthquake (December 17, 1992) [*Dziewonski et al.*, 1993] demon-

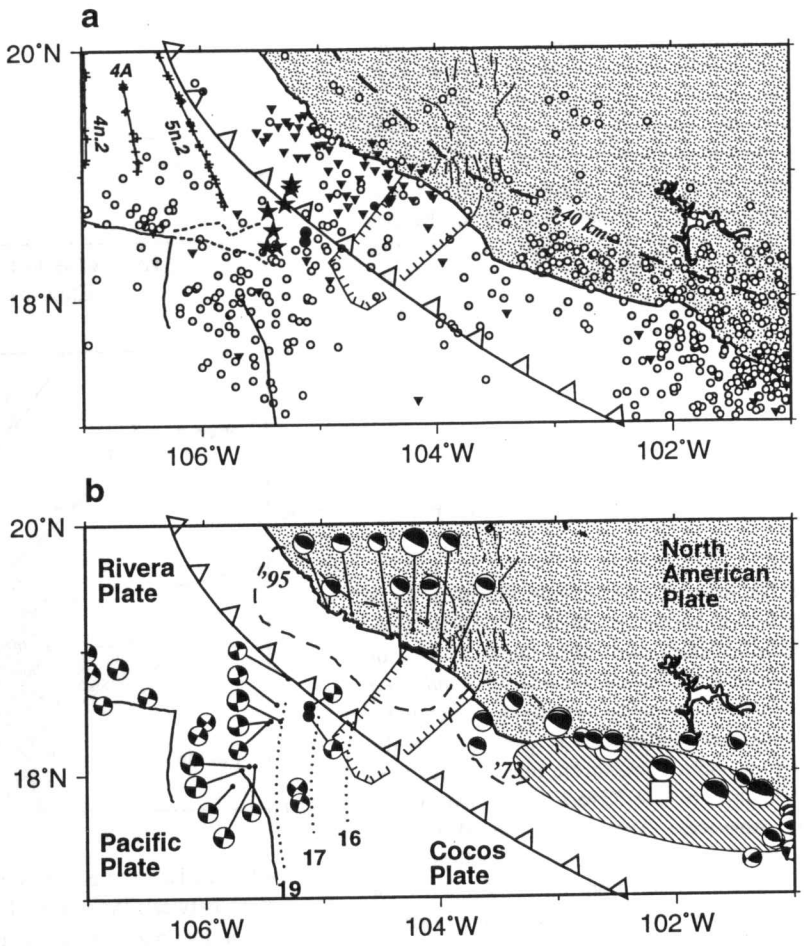

Figure 8. (a) Regional seismicity near the Rivera-Cocos plate boundary. Triangles show all earthquakes that occurred between October 5, 1995, and August 1996, thereby including all earthquakes related to the October 9, 1995, M_w = 8.0 earthquake. Open circles show all earthquakes shallower than 60 km that occurred between January 1967 and October 5, 1995. Stars designate the sequence of strike-slip earthquakes that were apparently triggered by the Manzanillo subduction earthquake. The two solid circles show the locations of two strike-slip earthquakes modeled by *Eissler and McNally* [1984]. The dashed line shows the 40 km depth contour for the subducting slabs [*Pardo and Suarez*, 1995]. Plus symbols define shipboard crossings of anomalies 4n.2, 4A, and 5n.2 [*Traylen*, 1995]. (b) Seismotectonics in the vicinity of the Rivera-Cocos deformation zone. The square and the hachured ellipse show the location and 2-D 95% confidence limits of the Rivera-Cocos rotation axis (Table 1c). Dotted lines show the CCW small circle paths followed by the Rivera plate about this pole. Numbers at the southern ends of the small circles are predicted Rivera-Cocos rates in millimeters per year. Earthquake focal mechanisms are compiled from *Eissler and McNally* [1984], *Reyes et al.* [1979], *Pardo and Suarez* [1995], and the Harvard centroid moment tensors for the period January 1977 through July 1996 [e.g., *Dziewonski et al.*, 1990]. Dashed lines outline the rupture zones of the M_s = 7.5 Colima earthquake on January 30, 1973 and the M_w = 8.0 Manzanillo earthquake on October 9, 1995.

strate that left-lateral slip is locally accommodated along one or more north trending faults (Figure 8b).

The kinematic prediction of south directed motion of the Rivera plate relative to a fixed Cocos plate (Figures 8b and 9) agrees well with the observations of north trending, left-lateral slip between these two plates and indicates that Rivera-Cocos motion is accommodated through sinistral shearing along one or more faults within a north trending shear zone (Figure 9b). Although the kinematic model places no constraints on the width of the shear zone or distribution of slip within it, various observations hint at its geographic limits. The northwestern limit appears to be marked by the southeast end of anomaly 5n.2 (at 18.75°N, 105.9°W in Figure 8a) and the undeformed eastern end of the Rivera fracture zone, which terminates at ~18.4°N, 105.5°W (Figures 2 and 5) [*Bandy and Hilde*, 1996]. Neither of these features appears to be disrupted or rotated by discrete or distributed shear. The southern limit is presumably located north of ~16°N, which marks the approximate northern edge of rigid Pacific-Cocos motion.

Given the well-constrained prediction of ~20 mm yr^{-1} of Rivera-Cocos motion near the center of their diffuse boundary, the lack of morphologic evidence for significant faulting in the vicinity of their diffuse boundary [*Bourgois et al.*,

1988a] is somewhat puzzling. To resolve this apparent contradiction, *Bandy et al.* [1996] suggests that the Rivera-Cocos rotation axis may lie near the morpho-tectonic center of the diffuse Rivera-Cocos plate boundary. By implication, little or no Rivera-Cocos motion would be predicted in the vicinity of the plate boundary. Such a pole location lies far outside the 2-D 95% confidence limits of the best fitting Rivera-Cocos rotation (Figures 6 and 8b), which indicates that models that postulate little or no Rivera-Cocos motion in the vicinity of their plate boundary violate the unambiguous kinematic constraints described above. This topic is treated next.

Discussion

Distinguishing Between Alternative Models of Rivera-Cocos Motion

On the basis of the lack of morphologic evidence for a distinct Rivera-Cocos plate boundary, *Bandy* [1992] first proposed that motion between these two plates might be slow or absent in the vicinity of their diffuse boundary. *Bandy and Pardo* [1994] pursue this line of reasoning by examining whether slow Rivera-Cocos divergence is permitted in the vicinity of the El Gordo graben within the uncertainties they estimate for the velocities of the Rivera and Cocos plates relative to North America. They conclude that their kinematic data are inconsistent with such a conclusion but that Rivera-Cocos motion could nonetheless be slow or absent if the velocities of one or both plates have changed significantly since ~1 Ma. In support of an inference of slow or no Rivera-Cocos motion, *Kostoglodov and Bandy* [1995] conclude that a suite of independent relationships between maximum earthquake magnitudes, maximum seismic depths, ages of subducting slabs, and plate convergence rates all favor a model in which the rate of Rivera plate convergence beneath North America is approximately the same as that of the Cocos plate in the vicinity of the El Gordo graben. Their "high-rate" model thus predicts a maximum Rivera-North America rate of ~50 mm yr^{-1} (Figure 9b).

Stripped to its essence, the question of whether the Rivera and Cocos plates have moved relative to each other along their boundary since 0.78 Ma requires solving for the rotations that best represent Pacific-Rivera and Pacific-Cocos motion and then examining whether the linear velocities predicted by the corresponding angular velocities at a common location along the Rivera-Cocos boundary differ significantly (Figure 9a). Proper treatment of the data uncertainties is essential because the uncertainties dictate the level at which two models can be distinguished from each other. We find that the inference of zero or slow present-day motion between the Rivera and Cocos plates in the vicinity of their plate boundary is strongly rejected by the numerous, unambiguous magnetic anomaly and especially fracture zone crossings from the Pacific-Rivera and Pacific-Cocos plate boundaries (Figure 9a). To examine whether these kinematic data ever yield a model that predicts negligible present-day Rivera-Cocos motion near the center of their diffuse boundary, we iteratively estimated the velocity of the Cocos plate relative to the Rivera plate at 18.4°N, 105.3°W while randomly perturbing the many kinematic data within bounds

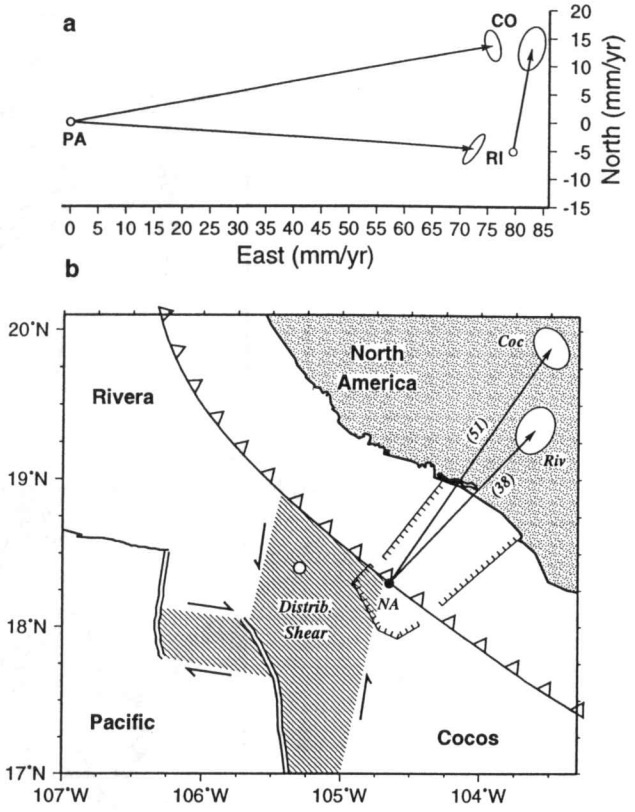

Figure 9. (a) Linear velocities and 2-D 95% confidence limits for motion between the Cocos, Rivera, and Pacific plates at the location of the open circle in Figure 9b. The Rivera-Cocos velocity vector is offset to the right for clarity. (b) Postulated model for seafloor deformation between the Rivera and Cocos plates. Paired, one-sided arrows parallel the Rivera-Cocos and Pacific-Rivera velocities. The sinistral and dextral shear zones are roughly defined by seismicity west of the trench. Velocities of the Rivera and Cocos plates relative to North America are also shown with their 2-D 95% confidence limits. The rates in millimeters per year are enclosed in parentheses.

specified by their probability density functions (see above). For 1000 iterations, the rates ranged from 15 to 23 mm yr^{-1} and the azimuths ranged from N01°E to N21°E. The probability of a Rivera-Cocos rate slower than 15 mm yr^{-1} at this location is thus less than 0.1%. This implies that the probability of slow or no motion at this location is vanishingly small.

In light of this result and the corroborating seismologic evidence described above, we are unpersuaded that the lack of morphologic evidence for faults that accommodate motion between the Rivera and Cocos plates must be interpreted as evidence that motion between the two plates is slow or zero in the vicinity of their diffuse boundary [*Bandy et al.*, 1996]. We would not expect the morphologic signature of distributed shear to be obvious for two reasons. First, distributed shear has produced apparent rotations exceeding 45° at other diffuse plate boundaries without creating visible faults in the direction of shear [e.g., *Kleinrock and Hey*, 1989; *Wilson*, 1989]. If the offshore boundary between the Rivera and Cocos plates is a zone of uniform simple shear at least 50 km

wide, the strain rate will be low enough that the maximum apparent rotation rate will be about 20°/Myr. Nearly all of the seafloor in the shear zone is subducted within 1.5-2 Myr of its birth at the spreading center, thereby leaving little time to leave a marked signature in the seafloor. Second, distributed shear can generally only be recognized in cases where the tectonic setting is understood well enough to know the original trend of the bathymetric fabric. Seafloor near the eastern end of the Rivera fracture zone has a complex and incompletely understood tectonic history [*Bandy et al.*, 1996]. The effects of distributed shear might therefore be difficult to recognize, particularly in light of the small angle between the predicted shear direction and the nearly N-S seafloor fabric that prevails in at least part of the diffuse plate boundary.

We also considered the possibility that present-day motion between the Rivera and Cocos plates might be much slower than the 0.78 Ma average. This is relevant to the interpretation of more instantaneous measures of Rivera-Cocos motion such as seismicity, but does not affect the kinematic requirement of ~15 km of N-S sinistral offset within the Rivera-Cocos boundary since 0.78 Ma. A large decrease in the Rivera-Cocos rate would require some combination of a simultaneous decrease in both the Pacific-Rivera and Pacific-Cocos spreading rates and/or a decrease in the angle between the Pacific-Rivera and Pacific-Cocos slip directions (Figure 9a). Such a model seems highly unlikely for the following reasons. First, evidence from swath mapping surveys of Pacific-Cocos and Pacific-Rivera seafloor younger than 1 Ma suggests that the angle between the Pacific-Rivera and Pacific-Cocos slip directions has increased since 0.78 Ma, which implies that the Rivera-Cocos rate has also increased. Along the Pacific-Rivera rise, the abyssal hill fabric appears to have rotated clockwise by several degrees since 0.78 Ma [*Lonsdale*, 1995]. Similarly, abyssal hill orientations along the Pacific-Cocos rise from ~9°N to 17°N have changed several degrees counter-clockwise since 1 Ma [*Perram and Macdonald*, 1990; *Edwards et al.*, 1991; *Carbotte and Macdonald*, 1992; *Weiland and Macdonald*, 1996]. Given that a decrease in the angle between Pacific-Rivera and Pacific-Cocos slip directions has not occurred, decreases of more than 50% in both the Pacific-Cocos and Pacific-Rivera spreading rates would be required to yield an instantaneous Rivera-Cocos rate slower than 10 mm yr^{-1} (Figure 9a). There is no evidence for such a dramatic simultaneous decrease in spreading rates. Stage spreading rates along the Pacific-Cocos spreading centers have remained nearly constant since ~5 Ma [*Wilson*, 1993c] and those along the Pacific-Rivera rise have varied by at most 20% over the same interval [*Traylen*, 1995].

Rivera-Cocos Motion at the El Gordo Graben and Beneath the Continental Margin

Nixon [1982] first suggested the idea that extension across the Colima graben within the North American plate is related to motion between the subducted Rivera and Cocos plates. The subsequent discoveries of the Manzanillo trough and El Gordo graben, which extend southwards offshore from the Colima graben, stimulated similar ideas about the connection between Rivera-Cocos motion and these extensional features [*Bourgois et al.*, 1988a; *Bandy*, 1992; *Bandy et al.*, 1995]. Below, we examine whether horizontal divergence between these two plates since 0.78 Ma could be responsible for any extension across these features.

At the latitude of the El Gordo graben, the Rivera-Cocos angular velocity predicts convergence everywhere west of 103.3°W, with rates that increase from 16±3 mm yr^{-1} at the western edge of the El Gordo graben to 19±3 mm yr^{-1} farther west (Figure 8b). Any extension across the graben cannot thus be attributed to horizontal divergence between the Rivera and Cocos plates. This suggests that the El Gordo graben is either not an extensional feature, that it no longer accommodates extension, or that it is only one of several structurally distinct elements that accommodate distributed Rivera-Cocos deformation.

Convergent motion between the Rivera and Cocos plates is also predicted beneath the Manzanillo trough and southern Colima graben (assuming that the subducted portion of the plate boundary lies beneath these features). Any extension within the North American plate above the subducting Rivera and Cocos slabs cannot therefore be attributed to horizontal divergence between the subducting slabs. Farther north, beneath the central and northern Colima grabens, the Rivera-Cocos rotation predicts that the subducting slabs have a small divergent component; however, even if the Rivera-Cocos boundary lies beneath these features, both subducting plates are significantly deeper than 40 km and are unlikely to affect the overlying continent (Figure 8a).

The model predictions indicate that any extension along the Manzanillo trough and Colima graben since 0.78 Ma cannot be easily explained by invoking a connection to divergence between the subducting Rivera and Cocos plates. We postulate that one or both of these features could be relicts of an earlier kinematic phase when the relative motion of the Rivera and Cocos plates may have had a divergent component beneath the continent, or that extension of the overlying continent could be a consequence of differential vertical motions of the subducting slabs [*Nixon*, 1982; *Bandy et al.*, 1995]. Rifting could also be a by-product of slow southeastward motion of a coastal sliver in response to slightly oblique subduction of the Cocos plate [*DeMets and Stein*, 1990]. Using epicentral information from *Pardo and Suarez* [1995] and the Harvard centroid-moment tensor catalog, we examined focal mechanisms of all shallow thrust earthquakes that have occurred since 1965 along the Middle America trench west of 100°W and found that 30 out of the 31 earthquakes that clearly record motion along the subduction thrust plane have horizontal slip directions counterclockwise from the convergence direction predicted by the Cocos-North America rotation. The slip directions are biased toward the trench-normal direction, thereby suggesting that Cocos-North America convergence is partitioned into trench-normal and trench-parallel components that are accommodated by different plate boundary structures, with the former being accommodated by the subduction zone and the latter resulting in slow southeastward motion of coastal regions relative to the interior of Mexico [*DeMets and Stein*, 1990]. *Kostoglodov and Bandy* [1995] further propose that slow northwestward motion of the crust northwest of the Colima graben (Figure 1) could result from slightly oblique subduction of the Rivera plate, which might also contribute to focused or distributed extension along or northwest of the Colima graben.

Conclusions

To describe the relative velocities of the Pacific, North American, Rivera, and Cocos plates since 0.78 Ma and test various hypotheses regarding deformation between these plates, we use numerous marine magnetic and bathymetric observations from the Pacific-Cocos, Pacific-Rivera, and Gulf rises to derive best fitting rotations and uncertainties. We demonstrate that seafloor spreading north of 22.0°N along the Pacific-Rivera rise occurs at a significantly different rate than is predicted by a rotation derived from magnetic anomaly crossings farther south along the rise. This supports a model in which seafloor north of several recently described rupture zones that extend southeast from the rise axis has detached from the Rivera plate and possibly sutured to North America [*Lonsdale*, 1995]. Our analysis of anomaly crossings immediately north and south of the Tamayo fracture zone places an upper bound of 4 mm yr^{-1} on any motion between the North American plate north of the eastern Tamayo fracture zone and seafloor just south of the fracture zone. We also corroborate previously published results that show there is a significant spreading deficit along the northernmost Pacific-Cocos rise. We attribute this deficit to deformation of the northern Cocos plate in response to diffuse motion between the Rivera and Cocos plates or deformation of the Pacific plate west of the rise axis, which seems less likely. We demonstrate that seafloor spreading along the Manzanillo spreading segment is indistinguishable from Pacific-Rivera motion since 0.78 Ma and thus incorporate anomaly crossings from the Manzanillo segment in our solution for Pacific-Rivera motion. The resulting well-constrained kinematic model predicts Pacific-Rivera and Pacific-Cocos velocities that differ by ~20±3 mm yr^{-1} along the Rivera-Cocos plate boundary. Focal mechanisms and distributions of strike-slip earthquakes within the diffuse Rivera-Cocos boundary agree well with the predictions of the new kinematic model and suggest that Rivera-Cocos motion is accommodated via distributed left-lateral motion across a north trending shear zone. Cocos-North America convergence rates along the Middle America trench since 0.78 Ma are ~10% faster than predicted by the NUVEL-1A model. This increase is attributable in part to an apparent increase in motion within the Pacific, Cocos, North America circuit since 3.16 Ma.

Acknowledgments. This work uses marine geophysical and seismologic data that were collected and archived through the concerted efforts of many people. Without their efforts, this work would not be possible. We thank Tanya Atwater, Bill Bandy, Bruce Luyendyk, and Will Sager for constructive comments and reviews, Goran Ekström for providing centroid moment-tensor solutions in advance of publication, and Ken Macdonald for sharing unpublished swath maps. Figures were produced using Generic Mapping Tool software [*Wessel and Smith*, 1991]. This work was funded by NSF grants EAR92-05083 (C.D.), OCE91-01748 (D.S.W.) and also benefited from support from the Wisconsin Alumni Research Foundation.

References

Anderson, J. G., S. K. Singh, J. M. Espindola, and J. Yamamoto, Seismic strain release in the Mexican subduction thrust, *Phys. Earth Planet. Inter., 58,* 307–322, 1989.

Argus, D. F., and R. G. Gordon, Pacific-North American plate motion from very long baseline interferometry compared with motion inferred from magnetic anomalies, transform faults, and earthquake slip vectors, *J. Geophys. Res., 95,* 17,315–17,324, 1990.

Atwater, T., and J. D. Mudie, Detailed near-bottom geophysical study of the Gorda Rise, *J. Geophys. Res., 78,* 8665–8686, 1973.

Baksi, A. K., A geomagnetic polarity time scale for the period 0–17 Ma, based on $^{40}Ar/^{39}Ar$ plateau ages for selected field reversals, *Geophys. Res. Lett., 20,* 1607–1610, 1993.

Baksi, A. K., V. Hsu, M. O. McWilliams, and E. Farrar, $^{40}Ar/^{39}Ar$ dating of the Brunhes-Matuyama geomagnetic field reversal, *Science, 256,* 356–357, 1992.

Bandy, W. L., Geological and Geophysical Investigation of the Rivera-Cocos Plate Boundary: Implications for Plate Fragmentation, Ph. D. dissertation, 195 pp., Tex. A&M Univ., College Station, 1992.

Bandy, W. and T. W. C. Hilde, Morphology and recent development history of the ridge propagation system located at 18°N, 106°W, *Geol. Soc. Am. Bull.*, in press, 1996.

Bandy, W., and M. Pardo, Statistical examination of the existence and relative motion of the Jalisco and southern Mexico blocks, *Tectonics, 13,* 755–768, 1994.

Bandy, W., C. Mortera-Gutierrez, J. Urrutia-Fucugauchi, and T. W. C. Hilde, The subducted Rivera-Cocos plate boundary: Where is it, what is it, and what is its relationship to the Colima rift?, *Geophys. Res. Lett., 22,* 3075–3078, 1995.

Bandy, W., T. W. C. Hilde, and C.-Y. Yan, The Rivera-Cocos plate boundary: Implications for Rivera-Cocos relative motion and plate fragmentation, *Geol. Soc. Am. Bull.*, in press, 1996.

Bassinot, F. C., L. D. Labeyrie, E. Vincent, X. Quidelleur, N. J. Shackleton, and Y. Lancelot, The astronomical theory of climate and the age of the Brunhes-Matuyama magnetic reversal, *Earth Planet. Sci. Lett., 126,* 91–108, 1994.

Bevington, P. R., and D. K. Robinson, *Data Reduction and Error Analysis for the Physical Sciences,* McGraw-Hill, New York, 1992.

Bourgois, J., et al., Fragmentation en cours du bord Ouest du Continent Nord Americain: Les frontieres sous-marines du Bloc Jalisco (Mexique), *C. R. Acad. Sci., Ser. I, 307,* 1121–1130, 1988a.

Bourgois, J., et al., La jonction orientale de la dorsale Est-Pacifique avec la zone de fracture de Rivera au large du Mexique, *C. R. Acad. Sci., Ser. I, 307,* 617–626, 1988b.

Cande, S. C., and D. V. Kent, Revised calibration of the geomagnetic polarity timescale for the Late Cretaceous and Cenozoic, *J. Geophys. Res., 100,* 6093–6095, 1995.

Carbotte, S., and K. Macdonald, East Pacific Rise 8°–10°30'N: Evolution of ridge segments and discontinuities from SeaMARC II and three-dimensional magnetic studies, *J. Geophys. Res., 97,* 6959–6982, 1992.

Chang, T., Estimating the relative rotation of two tectonic plates from boundary crossings, *J. Am. Stat. Assoc., 83,* 1178–1183, 1988.

Chang, T., J. Stock, and P. Molnar, The rotation group in plate tectonics and the representation of uncertainties of plate reconstructions, *Geophys. J. Int., 101,* 649–661, 1990.

Chase, C. G., The *n*-plate problem of plate tectonics, *Geophys. J. R. Astron. Soc., 29,* 117–122, 1972.

DeMets, C., A reappraisal of seafloor spreading lineations in the Gulf of California: Implications for the transfer of Baja California to the Pacific plate and estimates of Pacific-North America motion, *Geophys. Res. Lett., 22,* 3545–3548, 1995.

DeMets, C., and S. Stein, Present-day kinematics of the Rivera plate and implications for tectonics of southwestern Mexico, *J. Geophys. Res., 95,* 21,931–21,948, 1990.

DeMets, C., R. G. Gordon, D. F. Argus, and S. Stein, Current plate motions, *Geophys. J. Int., 101,* 425–478, 1990.

DeMets, C., R. G. Gordon, D. F. Argus, and S. Stein, Effect of recent revisions to the geomagnetic reversal timescale on estimates of current plate motions, *Geophys. Res. Lett., 21,* 2191–2194, 1994.

Dziewonski, A. M., G. Ekström, J. H. Woodhouse, and G. Zwart, Centroid-moment tensor solutions for October-December 1989, *Phys. Earth Planet. Inter., 62,* 194–207, 1990.

Dziewonski, A. M., G. Ekström, and M. P. Salganik, Centroid-moment tensor solutions for October-December 1992, *Phys. Earth Planet. Inter., 80,* 89–104, 1993.

Edwards, M. H., D. J. Fornari, A. Malinverno, W. B. F. Ryan, and J. Madsen, The regional tectonic fabric of the East Pacific Rise from 12°50'N to 15°10'N, *J. Geophys. Res., 96,* 7995–8017, 1991.

Eissler, H. K., and K. C. McNally, Seismicity and tectonics of the Rivera plate and implications for the 1932 Jalisco, Mexico, earthquake, *J. Geophys. Res., 89,* 4520–4530, 1984.

Fornari, D. J., D. G. Gallo, M. H. Edwards, J. A. Madsen, M. R. Perfit, and A. N. Shor, Structure and topography of the Siquieros transform fault system: Evidence for the development of intra-transform spreading centers, *Mar. Geophys. Res., 11,* 263–299, 1989.

Gallo, D. G., P. J. Fox, and K. C. Macdonald, A Sea Beam investigation of the Clipperton transform fault: The morphotectonic expression of a fast slipping transform boundary, *J. Geophys. Res., 91,* 3455–3467, 1986.

Goff, J. A., E. A. Bergman, and S. C. Solomon, Earthquake source mechanisms and transform fault tectonics in the Gulf of California, *J. Geophys. Res., 92,* 10,485–10,510, 1987.

Gordon, R. G., S. Stein, C. DeMets, and D. F. Argus, Statistical tests for closure of plate motion circuits, *Geophys. Res. Lett., 14,* 587–590, 1987.

Haines, A. J., and W. E. Holt, A procedure for obtaining the complete horizontal motions within zones of distributed deformation from the inversion of strain rate data, *J. Geophys. Res., 98,* 12,057–12,082, 1993.

Hellinger, S. J., The statistics of finite rotations in plate tectonics, Ph.D. thesis, 172 pp., Mass. Inst. of Technol., Cambridge, 1979.

Hilgen, F. J., Extension of the astronomically calibrated (polarity) time scale to the Miocene/Pliocene boundary, *Earth Planet. Sci. Lett., 107,* 349–366, 1991.

Jarrard, R. D., Terrane motion by strike-slip faulting of forearc slivers, *Geology, 14,* 780–783, 1986.

Kleinrock, M. C., and R. N. Hey, Migrating transform zone and lithospheric transfer at the Galapagos 95.5°W propagator, *J. Geophys. Res., 94,* 13,859–13,878, 1989.

Klitgord, K. D., and J. Mammerickx, Northern East Pacific Rise: Magnetic anomaly and bathymetric framework, *J. Geophys. Res., 87,* 6725–6750, 1982.

Kostoglodov, V., and W. Bandy, Seismotectonic constraints on the rate between the Rivera and North American plates, *J. Geophys. Res., 100,* 17,977–17,990, 1995.

Lonsdale, P., Structural patterns of the Pacific floor offshore of peninsular California, in *Gulf and Peninsular Provinces of the Californias*, edited by J. P. Dauphin and B. R. T. Simoneit, AAPG Mem. 47, 87–125, 1991.

Lonsdale, P., Segmentation and disruption of the East Pacific Rise in the mouth of the Gulf of California, *Mar. Geophys. Res., 17,* 323–359, 1995.

Macdonald, K. C., S. P. Miller, B. P. Luyendyk, T. M. Atwater, and L. Shure, Investigation of a Vine-Matthews magnetic lineation from a submersible: The source and character of marine magnetic anomalies, *J. Geophys. Res., 88,* 3403–3418, 1983.

Macdonald, K. C., et al., The East Pacific Rise and its flanks 8–18°N: History of segmentation, propagation and spreading direction based on SeaMARC II and Sea Beam studies, *Mar. Geophys. Res., 14,* 299–344, 1992.

McCaffrey, R., Oblique plate convergence, slip vectors, and forearc deformation, *J. Geophys. Res., 97,* 8905–8915, 1992.

McKenzie, D., and J. Jackson, The relationship between strain rates, crustal thickening, paleomagnetism, finite strain, and fault movements within a deforming zone, *Earth Planet. Sci. Lett., 65,* 182–202, 1983.

Ness, G. E., and M. W. Lyle, A seismo-tectonic map of the Gulf and peninsular province of the Californias, in *Gulf and Peninsular Provinces of the Californias*, edited by J. P. Dauphin and B. R. T. Simoneit, AAPG Mem. 47, 71–77, 1991.

Nixon, G. T., The relationship between Quaternary volcanism in central Mexico and the seismicity and structure of subducted oceanic lithosphere, *Geol. Soc. Am. Bull., 93,* 514–523, 1982.

Pardo, M., and G. Suarez, Shape of the subducted Rivera and Cocos plates in southern Mexico: Seismic and tectonic implications, *J. Geophys. Res., 100,* 12,357–12,374, 1995.

Perram, L. J., and K. C. Macdonald, A one-million-year history of the 11°45'N East Pacific Rise discontinuity, *J. Geophys. Res., 95,* 21,363–21,381, 1990.

Reyes, A., J. Brune, and C. Lomnitz, Source mechanism and aftershock study of the Colima, Mexico earthquake of January 30, 1973, *Bull. Seismol. Soc. Am., 69,* 1819–1840, 1979.

Richardson, R. M., and G. L. Cole, Plate reconstruction uncertainties using empirical probability density functions, *J. Geophys. Res., 96,* 10,391–10,400, 1991.

Royer, J.-Y., and T. Chang, Evidence for relative motions between the Indian and Australian plates during the last 20 Myr from plate tectonic reconstructions: Implications for the deformation of the Indo-Australian plate, *J. Geophys. Res., 96,* 11,779–11802, 1991.

Shackleton, N. J., A. Berger, and W. R. Peltier, An alternative astronomical calibration of the lower Pleistocene timescale based on ODP Site 677, *Trans. R. Soc. Edinburgh Earth Sci., 81,* 251–261, 1990.

Singh, S. K., L. Ponce, and S. P. Nishenko, The great Jalisco, Mexico, earthquakes of 1932: Subduction of the

Rivera plate, *Bull. Seismol. Soc. Am., 75,* 1301–1313, 1985.

Smith, D. E., et al., Tectonic motion and deformation from satellite laser ranging to LAGEOS, *J. Geophys. Res., 95,* 22,013–22,041, 1990.

Smith, W. H. F., and D. T. Sandwell, Marine gravity field from declassified Geosat and ERS-1 altimetry (abstract), *Eos Trans. AGU, 76 (46),*, Fall Meet. Suppl., F156, 1995.

Stein, S., and R. G. Gordon, Statistical tests of additional plate boundaries from plate motion inversions, *Earth Planet. Sci. Lett., 69,* 401–412, 1984.

Stock, J. M., and P. Molnar, Some geometrical aspects of uncertainties in combined plate reconstructions, *Geology, 11,* 697–701, 1983.

Traylen, S., Post-10 million year kinematics of the Rivera plate, M.S. thesis, 82 pp., University of Wisconsin-Madison, August, 1995.

Weiland, C. M., and K. C. Macdonald, Geophysical study of the East Pacific Rise 15°N-17°N: An unusually robust segment, *J. Geophys. Res., 101,* 20,257–20,275, 1996.

Wessel, P., and W. H. F. Smith, Free software helps map and display data, *Eos Trans. AGU, 72* (41), 441, 445–446, 1991.

Wilson, D.S., Deformation of the so-called Gorda plate, *J. Geophys. Res., 94,* 3065–3075, 1989.

Wilson, D. S., Confidence intervals for motion and deformation of the Juan de Fuca plate, *J. Geophys. Res., 98,* 16,053–16,071, 1993a.

Wilson, D. S., Relative motion of the Cocos, Nazca, and Pacific plates (abstract), *Eos Trans. AGU, 74 (43),* Fall Meet. Suppl., 585, 1993b.

Wilson, D. S., Confirmation of the astronomical calibration of the magnetic polarity timescale from sea-floor spreading rates, *Nature, 364,* 788–790, 1993c.

C. DeMets, 1215 W Dayton St., Department of Geology and Geophysics, University of Wisconsin - Madison, Madison, WI 53706. (email: chuck@geology.wisc.edu)

D. Wilson, Department of Geological Sciences, University of California, Santa Barbara, Santa Barbara, CA 93106. (email: wilson@rapa.geol.ucsb.edu)

(Received May 6, 1996; revised October 7, 1996;
accepted October 14, 1996.)